

Original papers

Wood species recognition through multidimensional texture analysis

Panagiotis Barmpoutis^{a,b,*}, Kosmas Dimitropoulos^b, Ioannis Barboutis^a, Nikos Grammalidis^b,
Panagiotis Lefakis^a

^a Faculty of Agriculture, Forestry and Natural Environment, School of Forestry, Aristotle University of Thessaloniki, 54124, Greece

^b Information Technologies Institute, Centre for Research and Technology Hellas, Thessaloniki 60361, Greece

ARTICLE INFO

Keywords:

Wood species recognition

Multidimensional texture analysis

ABSTRACT

Wood recognition is a crucial task for wood sciences and industries, since it leads to the identification of the anatomical features and physical properties of wood. Traditionally, the recognition process relies almost exclusively on human experts, who are based on various characteristics of wood, such as color, structure and texture. However, there are numerous types of wood species in the nature that are difficult to be identified even by experienced scientists. Towards this end, in this paper we propose a novel approach for automated wood species recognition through multidimensional texture analysis. By taking advantage of the fact that static wood images contain periodic spatially-evolving characteristics, we introduce a new spatial descriptor considering each wood image as a collection of multidimensional signals. More specifically, the proposed methodology enables the representation of wood images as concatenated histograms of higher order linear dynamical systems produced by vertical and horizontal image patches. The final classification of images, i.e., histogram representations, into wood species, is performed using a Support Vector Machines (SVM) classifier. For the evaluation of the proposed method, a dataset, namely “WOOD-AUTH”, consisting of more than 4200 wood images (from cross, radial and tangential sections of normal wood structure) of twelve common wood species existing in Greek territory, was created. Experimental results presented in this paper show the great potential of the proposed methodology, which, despite a small number of misclassification cases with regards to both anatomically similar and different species, outperforms a number of state of the art approaches, yielding a classification rate of 91.47% in wood cross sections.

1. Introduction

Numerous wood species with various anatomical characteristics and physical properties are used in industry for the manufacture of a wide range of products. Depending on their properties, different wood species have different usage and, as a consequence, there is a great variation in their price. The identification of wood species is a critical process, which not only leads to the proper utilization of woods, but also to the prevention of wood smuggling, as well as to the protection of several endangered tree species. Therefore, wood materials need to be examined thoroughly before their usage in industry, while their import into any country is prohibited without verification and species identification, due to the risk of carrying and transferring harmful micro-organisms that can threaten some native species (Voulgaridis et al., 2000).

The recognition of wood species is a laborious process, which is performed by experts, who attempt to distinguish the different species

based on their macroscopic and microscopic characteristics. Most of these characteristics can be observed in the transverse or cross section of woods, which is the plane perpendicular to the long axis of the trunk. The next most important surface for wood species recognition is the tangential section, which is the plane parallel to the long axis and tangent to the growth rings, while significant information can also be acquired by the radial section of wood, i.e., the vertical plane from the pith towards the bark (Bond and Hamner, 2002; Jones, 2016). Traditionally, experts use 10-power hand lens or magnifying glass to look the section that is being examined, while additional analysis of the physical characteristics of wood, such as the color, weight, smell and grain pattern can also help experts identify the correct species (Voulgaridis et al., 2000). Since no two pieces of wood, even of the same species, look exactly alike (Conners, 2011), wood species recognition is a difficult task, which is performed only by experienced specialists. For this reason, the needs of reducing the cost and time required for the training of experts and at the same time enhancing the accuracy of recognition

* Corresponding author at: Faculty of Agriculture, Forestry and Natural Environment, School of Forestry and Natural Environment, Aristotle University of Thessaloniki, 54124, Greece.

E-mail addresses: panbar@auth.gr (P. Barmpoutis), dimitrop@iti.gr (K. Dimitropoulos), jbarb@for.auth.gr (I. Barboutis), ngramm@iti.gr (N. Grammalidis), plefakis@for.auth.gr (P. Lefakis).

<https://doi.org/10.1016/j.compag.2017.12.011>

Received 18 January 2017; Received in revised form 8 December 2017; Accepted 9 December 2017

0168-1699/ © 2017 Elsevier B.V. All rights reserved.

has significantly increased the research interest on automatic wood species recognition methods.

Based on the recent advances in the area of computer vision and pattern recognition, most researchers have proposed image-based approaches attempting to address the problem either in microscopic or macroscopic scale. In the case of microscopic image analysis researchers aim to identify various microscopic wood features using CCD microscopes and use them as input to the classification system. More specifically, Yuliastuti and Suprijanto (2013) used CCD microscope with $50\times$ magnification and extracted a number of wood features by applying multichannel Gabor filter on the wood pores and concentric curves. Subsequently, an artificial neural network with back propagation method of multilayer perceptron (MLP) was used for the classification of 10 species of wood. On the other hand, Cavalin et al. (2013) proposed a method based on image segmentation and multiple feature sets for the identification of 112 species in a database containing microscopic images. Moreover, Gurau et al. (2013), captured microscopic images of $40\times$, $100\times$ and $200\times$ magnification and proposed an approach based on ImageJ, an image processing tool that was used for the separation and measurement of anatomical structures of wood sections and the estimation of statistical variables. The accuracy of recognition, however, relies heavily on the correct image segmentation, which remains an elusive goal in computer vision field so far (Wang et al., 2013). More recently Kobayashi et al. (2015) used X-rays for the mapping of woods in images, while other researchers have used spectrum analysis to identify wood species (Puttonen et al., 2010; Rojas et al., 2011). Nevertheless, identification techniques based on spectrum analysis are considered more expensive and they are more suitable to be executed in the laboratory (Zamri et al., 2016).

On the other hand, wood recognition approaches based on macroscopic images have recently attracted increased interest mainly due to their flexibility, simplicity and operability (Hu et al., 2015). To recognize wood species in macroscopic scale, researchers usually employ color analysis (Zhao, 2013) to extract color features, such as wood color variations, or they apply texture analysis aiming to identify various texture patterns corresponding to specific wood species. For the identification of such texture patterns, most of these approaches are based on the use of Gray Level Co-occurrence Matrices (GLCM). More specifically, Tou et al. (2007) proposed a method based on Gabor filters and co-occurrence matrices, while Khalid et al. (2008) extracted GLCM textural features and used an artificial neural network for the classification of wood species. On the other hand, Bremananth et al. (2009) introduced a wood species recognition method based on GLCM and a correlation technique, whereas Mohan et al. (2014) extracted GLCM features, such as entropy, standard deviation and correlation, from image blocks and applied correlation classification for the recognition of wood species. Furthermore, Barmpoutis and Lefakis (2016) used separately three channels of RGB images and GLCM textural features for the identification of wood species. Another forest species recognition method that combines color-based features and GLCM was presented by Paula et al. (2010). The authors composed a database of the Brazilian flora containing 22 different species and used a multilayer perceptron classifier for the identification of species. On the other hand, Prasetyo et al. (2010) presented a comparative study using several feature extraction methods, such as GLCM, Local Binary Patterns, Wavelet transformation, Rankletm Granulometry and Laws' Masks, and various classification techniques. More recently, Samanta et al. (2015) introduced a different approach using Haralick features, which are calculated from the co-occurrence matrix, and a multi-layer feed forward neural network trained with fast-back propagation to identify wooden and non-wooden surfaces.

The main limitation, however, of all above approaches is the fact that GLCM is rather sensitive to gray levels, i.e., a wood sample may be misclassified when wood image has different gray level intensity. To address the problem, Hafemann et al. (2014) investigated the usage of deep learning techniques, in particular Convolutional Neural Networks,

for texture classification in two forest species datasets, one with macroscopic images and another with microscopic images, while Hu et al. (2015) presented a method based on Scale Invariant Feature Transformation (SIFT) keypoints extracted from wood cross-section images and then used k-means clustering to calculate histograms. More recently, Zamri et al. (2016) introduced a new feature extractor, namely the improved-Basic Gray Level Aura Matrix (i-BGLAM), in order to accurately extract wood features from the wood texture and overcome the limitation of GLCM. In this paper, we propose a novel macroscopic method for wood species recognitions based on multidimensional texture analysis in order to further improve the classification accuracy. Inspired by the dynamic texture analysis techniques applied to video-based flame and smoke detection systems (Barmpoutis et al., 2014; Dimitropoulos et al., 2015; Dimitropoulos et al., 2016), in this paper, we consider each wood image as a collection of multidimensional spatially-evolving signals and we propose a methodology, which enables the representation of wood images as concatenated histograms of higher order linear dynamical systems produced by vertical and horizontal image patches. More specifically, this paper makes the following contributions:

- We propose a novel methodology for the modeling and recognition of wood species. The proposed methodology takes advantage of the fact that static wood images contain periodic spatially-evolving characteristics in each image channel. Towards this end, we introduce a new spatial descriptor by considering each wood image as a collection of multidimensional signals. More specifically, we divide each wood image into a number of horizontal and vertical multidimensional signals and we apply higher order linear dynamical systems analysis in order to extract their dynamics, i.e., the spatial dynamics of vertical and horizontal image patches. Subsequently, we create the vertical and horizontal histogram representations of the image by adopting a bag of systems approach and we concatenate the two histogram representations to form a spatial descriptor for each image. The final classification of images into wood species is performed using a multi-class SVM classifier.
- To evaluate the efficiency of the proposed methodology, we created a dataset, namely "WOOD-AUTH", consisting of more than 4200 images of normal wood structure from cross, radial and tangential sections of the twelve most common wood species existing in Greek territory. The experimental results show that the proposed methodology outperforms a number of state of the art approaches, yielding a classification rate of 91.47% in wood cross-sections images and 84.2% in wood radial and tangential sections.

The remainder of this paper is organized as follows: the next section presents the material used for the creation of the WOOD-AUTH dataset, as well as the proposed methodology for automated wood species recognition. Subsequently, experimental results are discussed, while finally conclusions are drawn in the last section.

2. Material and methods

2.1. Dataset description

In our research we focused mainly on coniferous woods and broadleaf woods, which are widely known as "softwoods" and "hardwoods" respectively, since most species of conifers have moderate or low densities, while those of most hardwoods have moderate, high or extremely high densities. More specifically, we created a dataset, namely "WOOD-AUTH", consisting of samples of normal wood structure of twelve wood species (three softwood species and nine hardwood species) that exist in Greek territory (Table 1). In particular, *Fagus sylvatica*'s natural habitat extends over a large part of Europe from southern Sweden to northern Sicily. The distribution of *Juglans regia* (walnut) is widely from the Balkans eastward to the Himalayas and

Table 1
Wood species.

Botanical name	Category	Characteristics
<i>Fagus sylvatica</i>	Diffuse-porous hardwood	Boundaries of growth rings and wood rays are visible to the naked eyes
<i>Juglans regia</i>	Semi-diffuse-porous hardwood	Growth rings are often visible to the naked eyes
<i>Castanea sativa</i>	Ring-porous hardwood	Growth rings are quite visible to the naked eyes
<i>Quercus cerris</i>	Ring-porous hardwood	Wide and quite visible wood rays
<i>Alnus glutinosa</i>	Diffuse-porous hardwood	Wide and little visible wood rays. Blurred growth rings
<i>Fraxinus ornus</i>	Ring-porous hardwood	Growth rings are often visible to the naked eyes
<i>Picea abies</i>	Softwood	Blurred boundaries of earlywood and latewood
<i>Pinus sylvestris</i>	Softwood	Resin canals are visible to the naked eyes. Abrupt transition from the earlywood to the latewood
<i>Ailanthus altissima</i>	Ring-porous hardwood	Large porous in the earlywood and large rays
<i>Robinia pseudoacacia</i>	Ring-porous hardwood	Visible wood rays to the naked eyes strong presence of growth rings
<i>Cupressus sempervirens</i>	Softwood	Discontinuous growth rings and unclear limits earlywood and latewood
<i>Platanus orientalis</i>	Diffuse-porous hardwood	Wide and visible wood rays and quite visible growth rings

southwest China. *Castanea sativa* is native to South Europe, North Africa, Southwestern Asia and is widely naturalized in west Europe. It is known that oaks fall into one of two categories: white oak and red oak. *Quercus cerris* belongs in the category of red oaks and it is native to the south east France and across to the Balkans and Turkey. It is widely planted in much of Europe. *Alnus glutinosa* is native to almost the whole of continental Europe. Its natural habitat is moist ground near rivers, ponds and lakes. *Fraxinus ornus* is naturally distributed in southern Europe and southwestern Asia, with populations in the mountainous areas of the Middle East. *Picea abies* is native in European Alps, the Balkan mountains, and the Carpathians, its range extending north to Scandinavia and merging with *Siberian spruce* in northern Russia. It is widely planted in British Isles and North America. *Pinus sylvestris* is the most widely distributed pine in the world and it is native range in Eurasia and can be found in many areas in the United States and Canada. *Ailanthus altissima* (tree-of-heaven) is native to Taiwan and central China. It was introduced and became widespread in Europe in the 1700s. *Robinia pseudoacacia* is native in North America and occurs in parts of South America, Europe, Asia, Africa and Australia. *Cupressus sempervirens* is native in Greece and it can be found in the entire Mediterranean region. Finally, *Platanus orientalis* is recognized in ancient Greek history and literature. Its natural distribution extends from the eastern Mediterranean and throughout the Middle East to south-eastern Siberia. Samples of normal wood structure from the above species were collected from different regions of Greece (e.g. Epirus, Macedonia, Thrace, Thessaly) with the aim of maximizing the diversity of the data and to render the identification of wood samples independent of different growth conditions. The total number of images from cross, radial and tangential wood sections in the dataset is 4272. We have to note here that the main objective of this research is the development of an algorithm, which will be able to recognize wood

species from macroscopic images that have not been taken by professional photographers under ideal shooting conditions. Wood images (Fig. 1) of “WOOD-AUTH” dataset were acquired at the Laboratory of Wood Technology of Forestry and Natural Environment School of Aristotle University of Thessaloniki, Greece and they were taken from distance of 15–20 cm using Nikon D3300 digital camera of 24 megapixels. All images have been cropped to size of 400×400 pixels.

2.2. Methodology

As we can see from Fig. 1, static wood images contain periodic spatially-evolving characteristics, i.e., successive, interrelated and repetitive patterns that are unique for each species. To exploit this information, in this paper we consider each wood image as a set of multidimensional signals (i.e., we take into account all image channels) evolving spatially towards horizontal and vertical direction. To do so, we follow a specific patching approach, which divides each wood image into overlapping vertical patches of size $n \times p \times m$ pixels (where n is the size of image, p indicates the size of patch and m is the number of image channels) as well as overlapping horizontal patches of size $p \times n \times m$ pixels as shown in Fig. 2. This procedure creates $n-p$ patches in each direction. It is worth mentioning that we don't apply any pre-processing step to enhance the quality of images and we don't convert the images to gray-scale, as is commonly done in GLCM-based approaches, which ignore thereby the dynamical information of image channels.

To classify each patch (horizontal or vertical), we represent the signal as a third order tensor and we apply a higher order linear dynamical systems analysis in order to extract both its appearance and dynamics information. This procedure is applied to each patch in two directions, i.e., left and right for the horizontal patches and top and

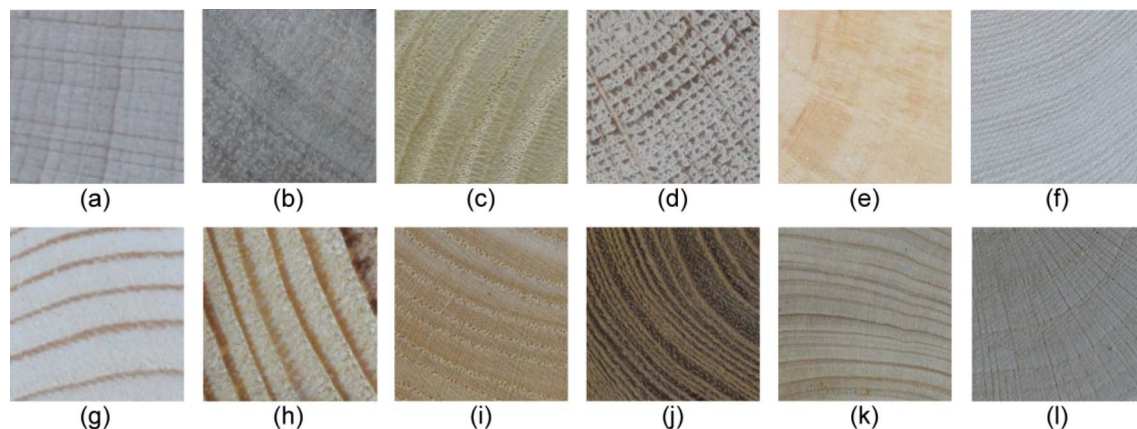


Fig. 1. Wood samples of database: (a) *Fagus sylvatica*, (b) *Juglans regia*, (c) *Castanea sativa*, (d) *Quercus cerris*, (e) *Alnus glutinosa*, (f) *Fraxinus ornus*, (g) *Picea abies*, (h) *Pinus sylvestris*, (i) *Ailanthus altissima*, (j) *Robinia pseudoacacia*, (k) *Cupressus sempervirens*, (l) *Platanus orientalis*.

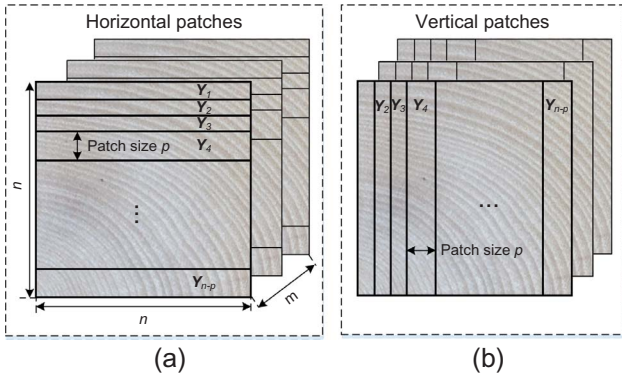


Fig. 2. Different orientations and sizes of patches for the proposed methodology: (a) vertical patches, (b) horizontal patches.

down for the vertical ones. Hence, for each patch we extract two descriptors, so we get $4n-4p$ descriptors in total for each image. Subsequently, we define two different codebooks, one for the horizontal and the other for the vertical patches, and we apply a bag of systems approach to create a histogram representation of wood image for each group of patches, i.e., horizontal and vertical. Each codebook consists of K codewords corresponding to the K representative patches. For each new image, we concatenate the vertical and horizontal histogram representations to create a new descriptor, V-H descriptor, and we classify it using an SVM classifier, as shown in Fig. 3.

2.3. Multidimensional texture analysis of wood image patches

In the case of a time-evolving data, the signal can be modeled by a first order ARMA process with white zero mean IID Gaussian input. More specifically, the stochastic modeling of both signal's dynamics and appearance is encoded by two stochastic processes, in which dynamics are represented as a time-evolving hidden state process $x(t) \in R^N$ and the observed data $y(t) \in R^d$ (e.g., for a video frame, d indicates the number of pixels in a frame $y(t)$) as a linear function of the state vector:

$$x(t+1) = Ax(t) + Bv(t) \quad (1)$$

$$y(t) = \bar{y} + Cx(t) + w(t) \quad (2)$$

where $A \in R^{N \times N}$ is the transition matrix of the hidden state, while $C \in R^{d \times N}$ is the mapping matrix of the hidden state to the output of the system. The quantities $w(t)$ and $Bv(t)$ are the measurement and process

noise respectively, with $w(t) \sim N(0, R)$ and $Bv(t) \sim N(0, Q)$, while $\bar{y} \in R^d$ is the mean value of the observation data. The LDS descriptor, $M = (A, C)$, contains both the appearance information of the observation data modeled by C , and its dynamics that are represented by A (Doretto et al., 2003).

Since static wood image patches can be considered as spatially-evolving multidimensional signals, we can adopt a similar approach in order to extract the appearance information and the dynamics of each image patch. Given a patch, let's consider for instance a horizontal patch (the proof for a vertical patch is straightforward) containing periodic spatially-evolving characteristics, the multidimensional spatial signal can be represented by tensor $Y \in R^{p \times n \times m}$, where p is the size of patch (in our experiments we set $p = 3$, since it gave us the best results), n is the size of image ($n = 400$ for all images in WOOD-AUTH dataset) and also the total number of samples i in each multidimensional signal (in the case of static wood images, the spatial samples $i = 1 \dots n$ play the role of time t in Eqs. (1) and (2)), while m indicates the dimension of the signal and is equal to the number of image channels, i.e., $m = 3$ for an RGB image.

For the estimation of the system parameters, i.e., A and C , several approaches have been proposed based either on EM algorithm or non-iterative subspace methods (Overschee and Moor, 1994). Since these approaches require high computational cost, a suboptimal method was proposed in (Doretto et al., 2003), according to which the columns of the mapping matrix C can be considered as an orthonormal basis, e.g., a set of principal components. Since in our case, the multidimensional signal of each wood image patch is represented by a tensor Y , instead of using principle components analysis, as proposed in (Doretto et al., 2003), we apply a higher order singular value decomposition (Kuo, 2013) to decompose the tensor:

$$Y = S \times_1 U_{(1)} \times_2 U_{(2)} \times_3 U_{(3)} \quad (3)$$

where $S \in R^{p \times n \times m}$ is the core tensor, while $U_{(1)} \in R^{p \times p}$, $U_{(2)} \in R^{n \times n}$ and $U_{(3)} \in R^{m \times m}$ are orthogonal matrices containing the orthonormal vectors spanning the column space of the matrix and \times_j denotes the j -mode product between a tensor and a matrix. Since the columns of the mapping matrix C of the stochastic process need to be orthonormal, we can easily choose one of the three orthogonal matrices of Eq. (3) to be equal to C . In addition, given the fact that the choice of matrices A , C and Q in Eqs. (1) and (2) is not unique, we can consider $C = U_{(3)}$ and

$$X = S \times_1 U_{(1)} \times_2 U_{(2)} \quad (4)$$

Hence, Eq. (3) can be reformulated as follows:

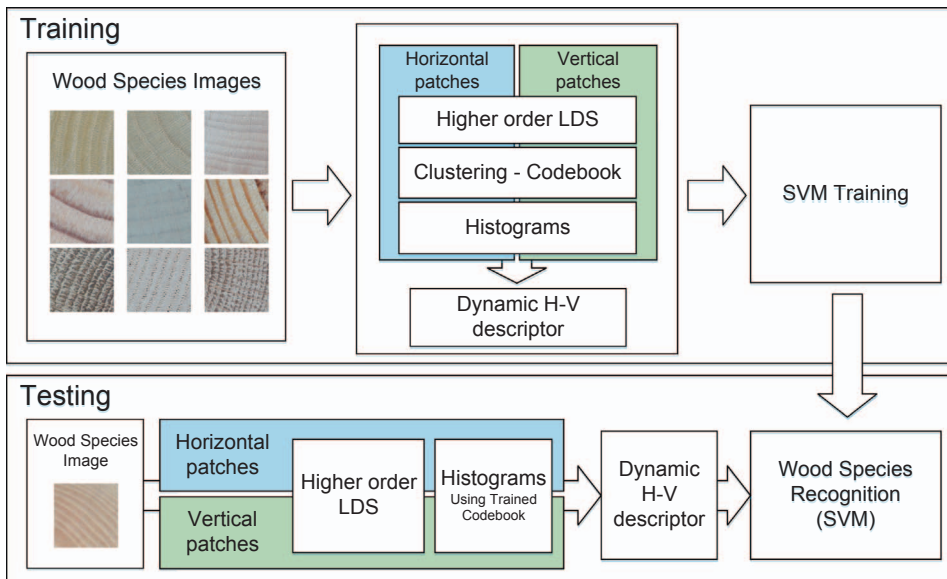


Fig. 3. The proposed methodology.

$$Y = X \times_3 C \Leftrightarrow Y_{(3)} = CX_{(3)} \quad (5)$$

where $Y_{(3)}$ and $X_{(3)}$ indicate the unfolding along the third dimension of tensors Y and X respectively and $X_{(3)} = [x(1), x(2), \dots, x(n)]$ are the estimated states of the system. If we define $X_1 = [x(2), x(3), \dots, x(n)]$ and $X_2 = [x(1), x(2), \dots, x(n-1)]$ the transition matrix A , containing the dynamics of the signal, can be easily computed by using least squares as:

$$A = X_2 X_1^T (X_1 X_1^T)^{-1} \quad (6)$$

After the estimation of the systems parameters, each wood image patch (horizontal or vertical) can be represented in each direction by the pair of matrices, A and C , i.e., the descriptor $M = (A, C)$.

2.4. The dynamic H-V descriptor

For each wood image, we estimate $4n-4p$ higher-order LDS (h-LDS) descriptors representing the appearance and dynamics information of each image patch (horizontal or vertical). In the next step, we define two different codebooks, one for the horizontal and the other for the vertical group of patches, and we apply a bag of systems approach to create a histogram representation of wood image for each group. Each codebook consists of K codewords corresponding to the K representative patches defined through a K-Medoid classification approach (Ravichandran et al., 2013). However, for the classification of the descriptors, we need first to define a similarity metric, i.e., a clustering approach applicable to the non-Euclidean space of h-LDSs in order to determine the similarity degree between two descriptors $M_1 = (A_1, C_1)$ and $M_2 = (A_2, C_2)$.

To overcome the problem, subspace angles between the two descriptors are initially calculated and then a Martin distance is used as a comparison metric (Cock and Moor, 2002). More specifically, for the estimation of the subspace angles between M_1 and M_2 , we need first to solve for P the Lyapunov equation $A^T P A - P = -C^T C$, where

$$P = \begin{bmatrix} P_{11} & P_{12} \\ P_{21} & P_{22} \end{bmatrix}, A = \begin{bmatrix} A_1 & 0 \\ 0 & A_2 \end{bmatrix}, C = [C_1 \ C_2] \quad (7)$$

The cosine of the subspace angles is calculated by the following formula:

$$\cos^2 \theta_i = i^{th} \text{ eigenvalue}(P_{11}^{-1} P_{12} P_{22}^{-1} P_{21}) \quad (8)$$

Based on the estimation of subspace angles, the Martin distance between M_1 and M_2 is defined as:

$$\text{Martin}_{distance}(M_1, M_2) = -\ln \prod_i \cos^2 \theta_i \quad (9)$$

Using Martin distance as a similarity metric and K -Medoids clustering, we can easily define the K representative codewords of each group and create a Term Frequency (TF) histogram representation of horizontal and vertical image patches. Subsequently, we concatenate the two histogram representations to form a spatial descriptor containing the appearance and dynamics information of all vertical and horizontal multidimensional signals in a wood image.

$$d_{H-V} = [h_H, h_V] = [h_{H1}, h_{H2}, \dots, h_{HK}, h_{V1}, h_{V2}, \dots, h_{VK}] \quad (10)$$

Finally, for the classification of $d_{H-V} \in R^{2K}$ descriptors into wood species classes, a multi-class Support Vector Machines (SVM) classifier is used, as shown in Fig. 4.

3. Results and discussion

In this section, we present a detailed experimental evaluation of our methodology using “WOOD-AUTH” dataset. The goal of this experimental evaluation is threefold: (a) Initially, we want to define the optimum set of parameters for our algorithm, (b) subsequently, we aim to show that the use of multidimensional data, i.e., RGB color images instead of gray scale images, and their representation as a third order

tensor improves significantly the classification accuracy and (c) finally, we want to demonstrate the superiority of the proposed algorithm in wood species recognition against a number of state of the art approaches. In all experimental results presented in this section, we have used the Leave-One-Out (LOO) cross-validation scheme, i.e., each time we leave out the testing wood image sample and we train the SVM classifier using all of the remaining wood images. This procedure is performed for every wood image sample in a cyclic manner, while the overall classification accuracy is estimated by averaging the accuracy of all iterations.

Fig. 5 illustrates wood species recognition results with various patch and codebook, i.e., number of clusters, sizes. More specifically, we run experiments with seven different codebook sizes (16, 32, 48, 64, 80, 96 and 128 codewords) and six different patch sizes (3, 5, 10, 16, 25 and 40 pixels), i.e., 42 experiments in total, using the wood cross section images of the “WOOD-AUTH” dataset. As we can easily see from Fig. 5c the proposed method, i.e., H-V descriptor, produces the best results for patch size of 3 pixels and codebook size of 96 codewords, yielding a detection rate of 91.47%. The classification rate, with the same parameters, for the histograms of horizontal and vertical patches is 84.85% and 80.44%, respectively, which shows that the multidimensional spatial signals in both directions contribute significantly to the classification process. The detection rate of the method using 80 and 128 codewords (for patch size equal to 3) is 91.32% and 91.40%, respectively, while the detection rate seems to be reduced when we increase the size of patches.

Having defined the best parameters of the algorithm, i.e., patch and codebook size, in the next experiment we aim to show that the use of multidimensional data, that is RGB color images instead of gray scale images, and their representation as a third order tensor improves significantly the classification accuracy, since in this case we take into account the hidden dynamics of spatial signals (horizontal and vertical) in all image channels. Fig. 6 presents experimental results using the original color wood images and the corresponding gray scale images of wood cross sections. As we can easily see, the use of multidimensional signals, represented as a third order tensor, outperforms the original LDS approach, which is based on principal components analysis and grayscale data, in all cases, i.e., horizontal, vertical and horizontal-vertical patches. Moreover, in order to have a more fair comparison against the original LDS descriptor, we decided to concatenate the RGB data into a vector representation. Again, experimental results show that the tensor representation of signals improves significantly the classification results achieving improvements up to 5.44% using both horizontal and vertical patches.

In Fig. 7, we present experimental results of the proposed method against a number of state of the art approaches for wood species recognition. More specifically, the proposed dynamic H-V descriptor is compared against: (i) standard GLCM method (Matlab, 2016), (ii) original BGLAM algorithm, (iii) i-BGLAM algorithm (Zamri et al., 2016), (iv) Deep Learning approach based on Convolutional Neural Networks as also used in (Hafemann et al., 2014) (in our experiments we trained the CNN network using as input the whole images instead of image patches due to the lower resolution of our images), (v) SIFT-based approach proposed in (Hu et al., 2015) and (vi) original LDS descriptor (Doretto et al., 2003). Experimental results show that the proposed method outperforms all state of the art approaches achieving improvements up to 2.94% in wood cross sections (H-V descriptor: 91.47%, i-BGLAM: 88.53%) and up to 9.13% in radial and tangential sections (H-V descriptor: 84.2%, i-BGLAM: 74.85%, CNN: 75.07%). As was expected all state of the art approaches improve the classification rate of GLCM, that is 63.40%, with the proposed method to provide an average detection rate of 82.02% for all wood sections (cross, radial and tangential sections). In general, cross wood sections provide higher detection rates for all methods, however, as we can see in Fig. 7 significant information can also be extracted from radial and tangential sections.

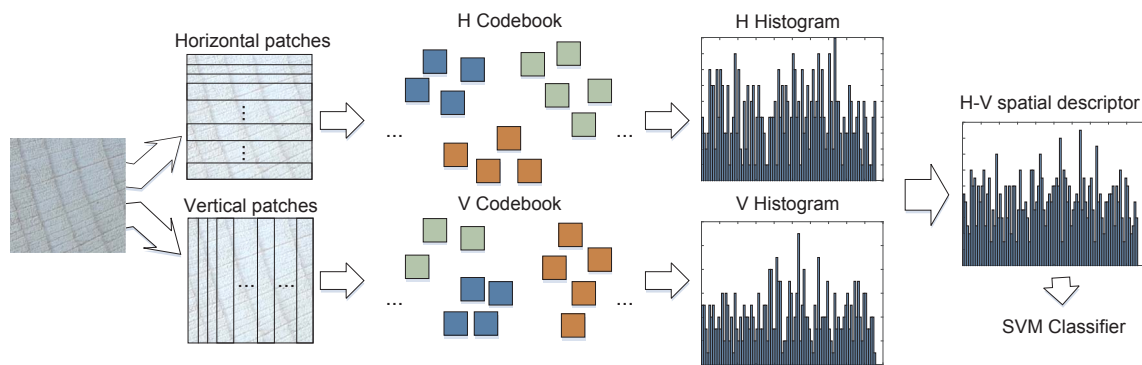


Fig. 4. The dynamic H-V descriptor.

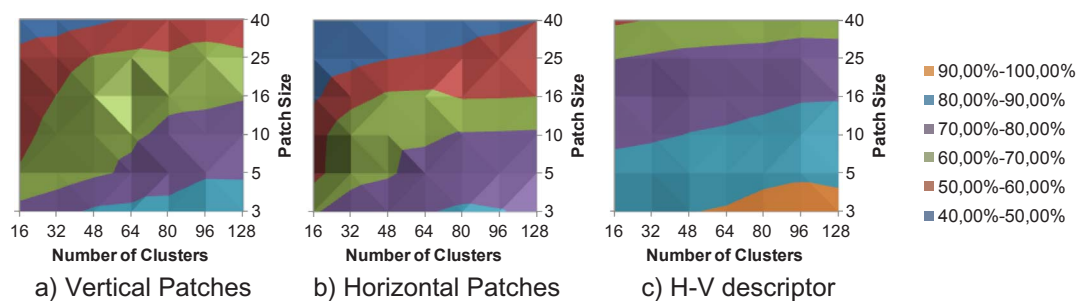


Fig. 5. Results of the proposed method for wood species recognition using h-LDS descriptors and (a) vertical patches, (b) horizontal patches, (c) blocks.

Figs. 8 and 9 illustrate the confusion matrices of the proposed method for the cross wood sections and the radial and tangential sections, respectively. In the case of cross wood sections, we can see that in most of the classes the classification rate is higher than 85%, with only this of *Quercus cerris* class to present lower detection rate, i.e., 79.63%. This is mainly due to the fact that both of *Quercus cerris* and *Castanea sativa* are ring-porous hardwood and some wood images of *Quercus cerris* are erroneously classified as *Picea abies* due to non-standard shooting conditions. Fig. 10a and b illustrates a characteristic example of *Castanea sativa* and *Quercus cerris*, where we can easily see that both wood species are porous hardwoods with quite visible growth rings. On the other hand, in the case of radial and tangential wood sections, we can see that only four classes (*Juglans regia*, *Quercus cerris*, *Alnus glutinosa* and *Fraxinus ornus*) present detection rates lower than 80%. More specifically, we observe some misclassifications between *Juglans regia* and *Castanea sativa* (Fig. 10c and d) due to the fact that both of them are porous hardwoods. Moreover, some wood species of *Quercus cerris* are

classified as *Castanea sativa* (Fig. 10e and f) since both of them are ring-porous hardwoods. However, we have to note here that the “WOOD-AUTH” dataset contains five different ring-porous species for which the overall classification accuracy is rather high, i.e., 90.33%. Moreover, for two of these species (*Ailanthus altissima* and *Robinia pseudoacacia*) there are no misclassification errors. This result shows that, in general, the proposed method can sufficiently recognize different ring-porous hardwoods, like elm or ash, as it takes into account the overall appearance characteristics of the images and their dynamics. Finally, some misclassifications between *Alnus glutinosa* and *Fagus sylvatica* (Fig. 10g and h) are explained by the fact that both of them are diffuse-porous hardwoods, while some images of *Fraxinus ornus* are incorrectly classified as *Fagus sylvatica* (Fig. 10i and j), mainly because both of them are porous hardwoods.

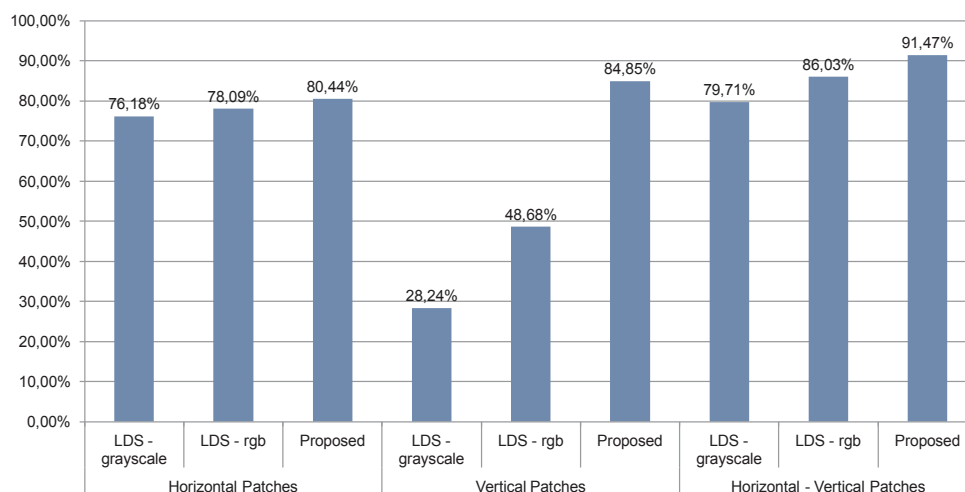


Fig. 6. Comparison of H-V descriptor against original LDS descriptor in grayscale and color wood images. (For interpretation of the references to colour in this figure legend, the reader is referred to the web version of this article.)

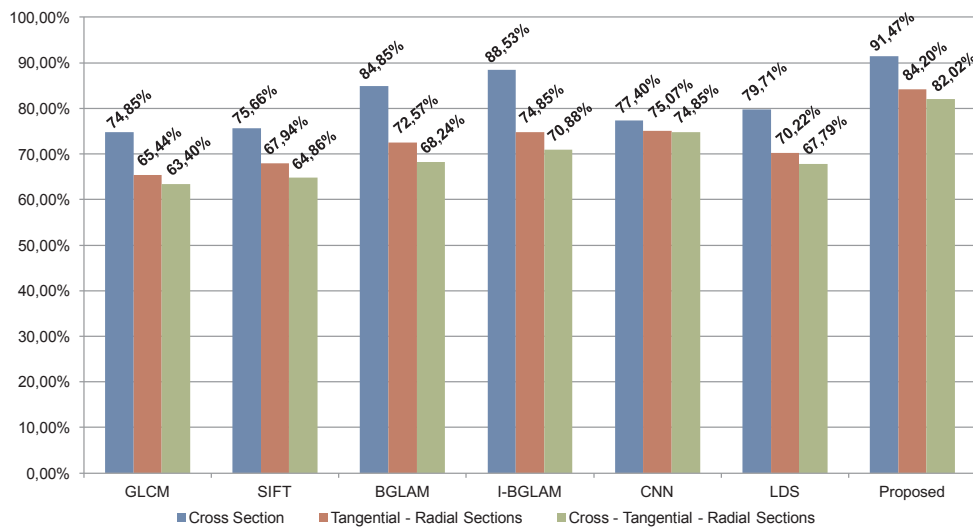


Fig. 7. Confusion matrix that represents True Positive and False Negative Rates for the late fusion approach using Vertical and Horizontal Patches.

	<i>Fagus sylvatica</i>	<i>Juglans regia</i>	<i>Castanea sativa</i>	<i>Quercus cerris</i>	<i>Alnus glutinosa</i>	<i>Fraxinus ornus</i>	<i>Picea abies</i>	<i>Pinus sylvestris</i>	<i>Ailanthus altissima</i>	<i>Robinia pseudoacacia</i>	<i>Cupressus sempervirens</i>	<i>Platanus orientalis</i>
<i>Fagus sylvatica</i>	89,90%	1,01%	2,02%	2,02%	1,01%	1,01%	1,01%	0,00%	0,00%	0,00%	0,00%	2,02%
<i>Juglans regia</i>	0,00%	95,65%	0,00%	4,35%	0,00%	0,00%	0,00%	0,00%	0,00%	0,00%	0,00%	0,00%
<i>Castanea sativa</i>	0,71%	0,00%	89,29%	4,29%	0,00%	2,14%	0,00%	0,00%	0,00%	1,43%	0,71%	1,43%
<i>Quercus cerris</i>	0,00%	0,00%	7,41%	79,63%	0,00%	0,00%	7,41%	0,00%	0,00%	1,85%	3,70%	0,00%
<i>Alnus glutinosa</i>	0,00%	0,00%	0,00%	0,00%	97,22%	0,00%	0,00%	0,00%	0,00%	0,00%	2,78%	0,00%
<i>Fraxinus ornus</i>	0,00%	0,00%	0,00%	0,00%	2,13%	87,23%	0,00%	0,00%	0,00%	0,00%	8,51%	2,13%
<i>Picea abies</i>	0,00%	0,00%	0,00%	0,00%	0,00%	3,03%	93,94%	3,03%	0,00%	0,00%	0,00%	0,00%
<i>Pinus sylvestris</i>	0,00%	0,00%	0,00%	0,00%	0,00%	0,00%	0,00%	100,00%	0,00%	0,00%	0,00%	0,00%
<i>Ailanthus altissima</i>	0,00%	0,00%	0,00%	0,00%	0,00%	0,00%	0,00%	0,00%	100,00%	0,00%	0,00%	0,00%
<i>Robinia pseudoacacia</i>	0,00%	0,00%	0,00%	0,00%	0,00%	0,00%	0,00%	0,00%	0,00%	100,00%	0,00%	0,00%
<i>Cupressus sempervirens</i>	0,00%	0,00%	3,13%	0,00%	1,56%	6,25%	0,00%	0,00%	1,56%	0,00%	87,50%	0,00%
<i>Platanus orientalis</i>	2,94%	1,47%	0,00%	0,00%	0,00%	1,47%	0,00%	0,00%	0,00%	0,00%	0,00%	94,12%

Fig. 8. The confusion matrix of the proposed method for the cross wood sections.

	<i>Fagus sylvatica</i>	<i>Juglans regia</i>	<i>Castanea sativa</i>	<i>Quercus cerris</i>	<i>Alnus glutinosa</i>	<i>Fraxinus ornus</i>	<i>Picea abies</i>	<i>Pinus sylvestris</i>	<i>Ailanthus altissima</i>	<i>Robinia pseudoacacia</i>	<i>Cupressus sempervirens</i>	<i>Platanus orientalis</i>
<i>Fagus sylvatica</i>	92,66%	0,00%	1,16%	1,16%	1,93%	2,32%	0,00%	0,00%	0,00%	0,00%	0,00%	0,77%
<i>Juglans regia</i>	2,00%	76,00%	10,00%	4,00%	4,00%	0,00%	0,00%	0,00%	0,00%	0,00%	0,00%	4,00%
<i>Castanea sativa</i>	2,40%	1,20%	84,80%	2,80%	1,20%	1,20%	0,40%	0,00%	0,40%	1,60%	2,80%	1,20%
<i>Quercus cerris</i>	5,10%	0,00%	12,24%	76,53%	0,00%	2,04%	0,00%	0,00%	0,00%	0,00%	1,02%	3,06%
<i>Alnus glutinosa</i>	6,62%	0,00%	1,47%	0,74%	79,41%	1,47%	2,21%	0,74%	0,74%	0,74%	2,94%	2,94%
<i>Fraxinus ornus</i>	12,61%	0,00%	6,31%	0,90%	0,00%	74,77%	0,00%	0,00%	0,00%	0,00%	2,70%	2,70%
<i>Picea abies</i>	2,53%	0,00%	1,27%	0,00%	3,80%	3,80%	84,81%	0,00%	1,27%	0,00%	2,53%	0,00%
<i>Pinus sylvestris</i>	0,00%	0,00%	5,36%	1,79%	1,79%	0,00%	0,00%	85,71%	0,00%	0,00%	5,36%	0,00%
<i>Ailanthus altissima</i>	1,82%	3,64%	9,09%	0,00%	0,00%	0,00%	0,00%	0,00%	80,00%	3,64%	1,82%	0,00%
<i>Robinia pseudoacacia</i>	1,01%	0,00%	4,04%	1,01%	1,01%	1,01%	0,00%	2,02%	1,01%	87,88%	1,01%	0,00%
<i>Cupressus sempervirens</i>	0,00%	0,00%	5,59%	0,00%	3,50%	1,40%	0,00%	0,70%	1,40%	0,00%	87,41%	0,00%
<i>Platanus orientalis</i>	3,33%	1,67%	5,00%	0,00%	2,50%	0,83%	0,00%	1,67%	1,67%	0,00%	0,83%	82,50%

Fig. 9. The confusion matrix of the proposed method for the radial and tangential wood sections.

4. Conclusions

In this paper we presented a novel approach for automated wood species recognition through multidimensional texture analysis. By taking advantage of the fact that static wood images contain periodic spatially-evolving characteristics, we introduced a new spatial descriptor considering each wood image as a collection of multi-dimensional signals. Subsequently, we used higher order linear dynamical systems and a bag of systems approach in order to represent wood images as concatenated histograms produced by vertical and horizontal image patches. To evaluate the efficiency of the proposed methodology,

we created a new dataset consisting of more than 4200 wood images of twelve different wood species existing in Greek territory. As we showed in the experimental results, the proposed methodology outperforms a number of the state of the art approaches. Moreover, in our study we showed that images containing wood cross sections provide higher classification rates than radial and tangential sections. Some misclassifications that were observed, between anatomically different wood species, can be explained by the fact that the purpose of this study was to develop a method that can use images obtained by non-professional photographers and under not ideal shooting conditions. Additionally, in the future, we aim to investigate various data fusion

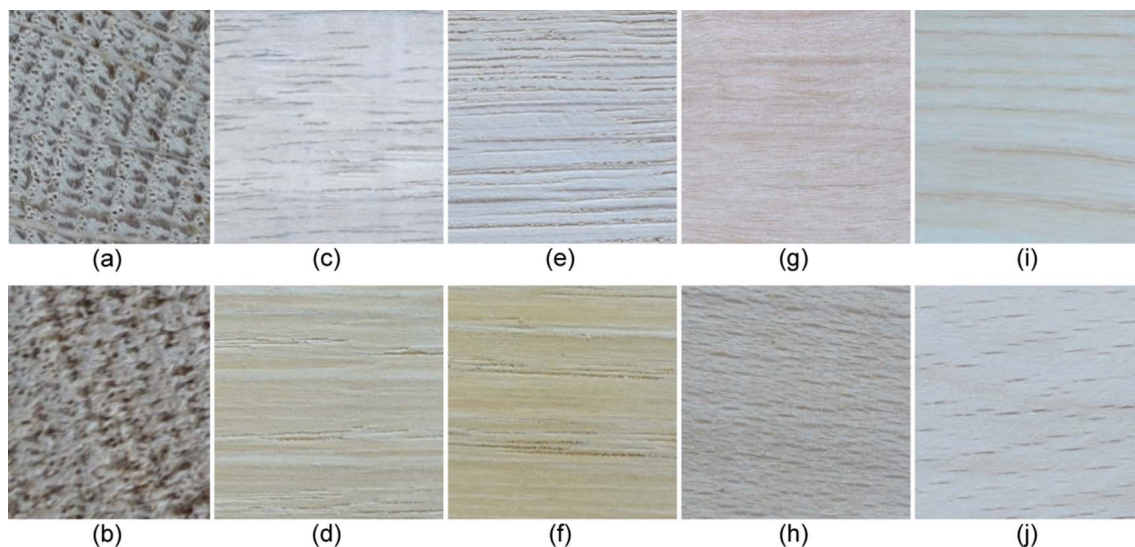


Fig. 10. Similarities of different wood species: (i) in cross section. (a) *Quercus cerris*, (b) *Castanea sativa*, (ii) in radial and tangential sections. (c) *Juglans regia*, (d) *Castanea sativa*, (e) *Quercus cerris*, (f) *Castanea sativa*, (g) *Alnus glutinosa*, (h) *Fagus sylvatica*, (i) *Fraxinus ornus*, (j) *Fagus sylvatica*.

approaches in order to improve the accuracy of our method by combining classification results of wood cross section images with those of radial and tangential sections. Finally, further experiments could be performed, using both macroscopic and microscopic images to extend the proposed methodology for species identification of the same genus, such as extremely similar wood species that produce the same commercial timber according to the standard EN 13556:2003 (Round and sawn timber. Nomenclature of timbers used in Europe).

References

- Barmpoutis, P., Dimitropoulos, K., Grammalidis, N., 2014. Smoke detection using spatio-temporal analysis, motion modeling and dynamic texture recognition. In: Proceedings of the 22nd European Signal Processing Conference, pp. 1078–1082.
- Barmpoutis, P., Lefakis, P., 2016. Development of mathematical model for automatic recognition of Greek wood species (in Greek with English abstract). In: Proceedings of the 8th International Week Dedicated to Maths 2016, Hellenic Mathematical Society, Thessaloniki, pp. 241–251.
- Bremananth, R., Nithya, B., Sai Priya, R., 2009. Wood Species Recognition Using GLCM and Correlation. In: Proceedings of the 2009 International Conference on Advances in Recent Technologies in Communication and Computing, pp. 615–619.
- Bond, B., Hamner, P., 2002. Wood identification for hardwood and softwood species native to Tennessee. University of Tennessee Extension, Knoxville, USA. [online 24 November 2016] URL: < http://nforestry.info/ut-extension/wood_identification/pb1692.pdf > .
- Cavalin, P.R., Kapp, M.N., Martins, J., Oliveira, L.E., 2013. A multiple feature vector framework for forest species recognition. In: Proceedings of the 28th Annual ACM Symposium on Applied Computing, pp. 16–20. <http://dx.doi.org/10.1145/2480362.2480368>.
- Cock, D.K., Moor, D.B., 2002. Subspace angles between ARMA models. Syst. Control Lett. 46 (4), 265–270. [http://dx.doi.org/10.1016/S0167-6911\(02\)00135-4](http://dx.doi.org/10.1016/S0167-6911(02)00135-4).
- Conners, T., 2011. The basics of wood identification. Kentucky Woodlands Mag. 6 (1), 4–6.
- Dimitropoulos, K., Barmpoutis, P., Grammalidis, N., 2016. Higher order linear dynamical systems for smoke detection in video surveillance applications. IEEE Trans. Circuits Syst. Video Technol. <http://dx.doi.org/10.1109/TCSVT.2016.2527340>.
- Dimitropoulos, K., Barmpoutis, P., Grammalidis, N., 2015. Spatio-temporal flame modeling and dynamic texture analysis for automatic video-based fire detection, IEEE Trans. Circuits Syst. Video Technol. (TCSVT), 25 (2), 339–351. <http://dx.doi.org/10.1109/TCSVT.2014.2339592>.
- Doretto, G., Chiuso, A., Wu, Y., Soatto, S., 2003. Dynamic textures. Int. J. Comput. Vision 51 (2), 91–109. <http://dx.doi.org/10.1023/A:1021669406132>.
- Gurau, L., Timar, M.C., Porjan, M., Ioras, F., 2013. Image processing method as a supporting tool for wood species identification. Wood Fiber Sci. 45 (3), 303–313.
- Hafemann, L.G., Oliveira, L.S., Cavalin, P.R., 2014. Forest species recognition using deep convolutional neural networks. Proc. Int. Conf. Pattern Recognition 1103–1107. <http://dx.doi.org/10.1109/ICPR.2014.199>.
- Hu, S., Ke, L., Bao, X., 2015. Wood species recognition based on SIFT keypoint histogram. In: Proceedings of the 8th International Congress on Image and Signal Processing, pp. 702–706. <http://dx.doi.org/10.1109/CISP.2015.7407968>.
- Jones, D., 2016. Basic guide to identification of hardwoods and softwoods using anatomical characteristics. Mississippi State University Extension, USA. [online] URL: < <http://extension.msstate.edu/sites/default/files/publications/publications/p2606.pdf> > .
- Khalid, M., Lee, E.L.Y., Yusof, R., Nadaraj, M., 2008. Design of an intelligent wood species recognition system. Int. J. Simulat. Syst. Sci. Technol. 9 (3), 9–19.
- Kobayashi, K., Akada, M., Torigoe, T., Imazu, S., Sugiyama, J., 2015. Automated recognition of wood used in traditional Japanese sculptures by texture analysis of their low-resolution computed tomography data. J. Wood Sci. 61 (6), 630–640. <http://dx.doi.org/10.1007/s10086-015-1507-6>.
- Kuo, T., 2013. Higher order SVD: theory and algorithms. [online 20 November 2016] URL: < <http://citeseerx.ist.psu.edu/> > .
- Matlab graycomatrix, 2016. The MathWorks, Inc., Natick, Massachusetts, United States. [online 5 November 2016] URL: < <https://www.mathworks.com/help/images/ref/graycomatrix.html> > .
- Mohan, S., Venkatachalapathy, K., Sudhakar, P., 2014. An intelligent recognition system for identification of wood species. J. Comput. Sci. 10 (7), 1231–1237. <http://dx.doi.org/10.3844/jcsp.2014.1231.1237>.
- Overschee, V.P., Moor, D.B., 1994. N4SID: subspace algorithms for the identification of combined deterministic-stochastic systems. Automatica 30 (1), 75–93. [http://dx.doi.org/10.1016/0005-1098\(94\)90230-5](http://dx.doi.org/10.1016/0005-1098(94)90230-5).
- Paula, P.L., Oliveira, L.S., Brito Jr., A.S., Sabourin, R., 2010. Forest species recognition using color-based features. Proc. Int. Conf. Pattern Recognition 4178–4181. <http://dx.doi.org/10.1109/ICPR.2010.1015>.
- Prasetyo, K.M., Yusof, R., Meriaudeau, F., 2010. A comparative study of feature extraction methods for wood texture classification. In: Proceedings of the Sixth International Conference on Signal-Image Technology and Internet-Based Systems, pp. 23–29. <http://dx.doi.org/10.1109/SITIS.2010.15>.
- Puttonen, E., Suomalainen, J., Hakala, T., Räikkönen, E., Kaartinen, H., Kaasalainen, S., Litkey, P., 2010. Tree species classification from fused active hyperspectral reflectance and LIDAR measurements. For. Ecol. Manage. 260 (10), 1843–1852. <http://dx.doi.org/10.1016/j.foreco.2010.08.031>.
- Ravichandran, A., Chaudhry, R., Vidal, R., 2013. Categorizing dynamic textures using a bag of dynamical systems. Trans. Pattern Anal. Mach. Intell. 35 (2), 342–353. <http://dx.doi.org/10.1109/TPAMI.2012.83>.
- Rojas, J.A.M., Alpuente, J., Postigo, D., Rojas, I.M., Vignote, S., 2011. Wood species identification using stress-wave analysis in the audible range. Appl. Acoust. 72 (12), 934–942. <http://dx.doi.org/10.1016/j.apacoust.2011.05.016>.
- Samanta, S., Kundu, D., Chakraborty, S., Dey, N., Gaber, T., Hassanien, A.E., Kim, T.H., 2015. Wooden surface classification based on Haralick and the neural networks. In: Proceedings of the Fourth International Conference on Information Science and Industrial Applications, pp. 33–40. <http://dx.doi.org/10.1109/ISI.2015.20>.
- Tou, J.Y., Lau, P.Y., Tay, Y.H., 2007. Computer vision based wood recognition system. In: Proceedings of the International Workshop on Advanced Image Technology.
- Voulgaridis, I., Pasialis, K., Vasileiou, V., 2000. In: Wood identification. (Academic press ed.) Aristotle University of Thessaloniki, Greece, pp. 1–20.
- Wang, H.J., Zhang, G.Q., Qi, H.N., 2013. Wood recognition using image texture features. Plos One J. 8 (10), 1–12. <http://dx.doi.org/10.1371/journal.pone.0076101>.
- Yuliastuti, E., Suprijanto, S.R., 2013. Compact computer vision system for tropical wood species recognition based on pores and concentric curve. In: Proceedings of the 3rd International Conference on Instrumentation Control and Automation, pp. 198–202. <http://dx.doi.org/10.1109/ICA.2013.6734071>.
- Zamri, M.I.P., Cordova, F., Khairuddin, A.S.M., Mokhtar, N., 2016. Tree species classification based on image analysis using Improved-Basic Gray Level Aura Matrix. Comput. Electron. Agric. 124, 227–233. <http://dx.doi.org/10.1016/j.compag.2016.04.004>.
- Zhao, P., 2013. Robust wood species recognition using variable color information. Optik – Int. J. Light Electron Optics 124 (17), 2833–2836. <http://dx.doi.org/10.1016/j.jlloe.2012.08.058>.